Electronic Supplementary Material (ESI) for Energy & Environmental Science.

ELECTRONIC SUPPORTING INFORMATION

Cadmium-Free $CuInS_2$/ZnS Quantum Dots as Efficient and Robust Photosensitizers in combination with a Molecular Catalyst for Visible Light-Driven H_2 Production in Water

M. Sandroni, R. Gueret, K-D. Wegner, P. Reiss, J. Fortage,* D. Aldakov,* M.-N. Collomb*

Spectral properties of CIS/ZnS-GSH QDs (particles synthesis)

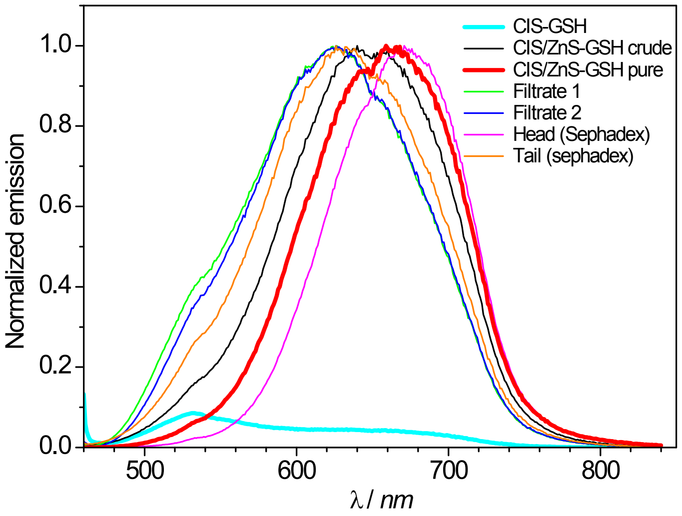

Figure S1. Normalized emission spectra of the different fractions collected during the particles synthesis and purification. “Filtrate 1” and “Filtrate 2” are the filtrates discarded after the centrifugal filtration steps, the “Head” and the “Tail” fractions are respectively the first and the last fraction obtained during purification by size-exclusion chromatography. The spectra indicate that a partial size selection was operated during purification 1 (centrifugal filtration), with a fraction of the smaller particles emitting at lower wavelengths which was discarded in the filtrate. Purification 2 (size exclusion chromatography on Sephadex column) also operated a size selection: indeed the particles collected after the main fraction (“Tail”) exhibited blue-shifted emission, while those collected before (“Head”) showed red-shifted luminescence.

Powder X-Ray Diffraction of CIS/ZnS-GSH QDs

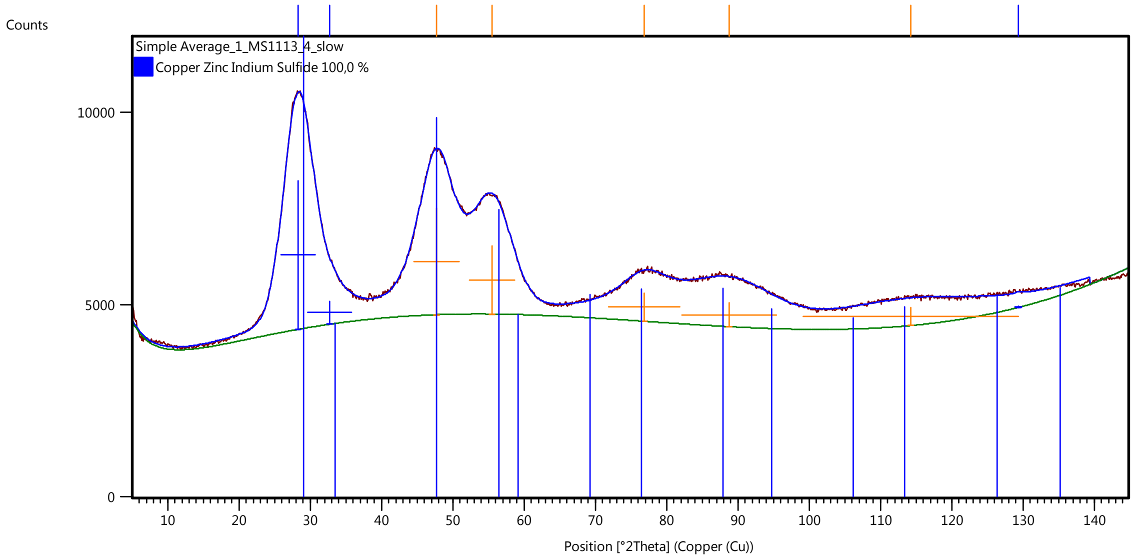

Figure S2. Powder X-Ray diffraction pattern of the CIS/ZnS-GSH QDs, compared with the reference (ICDD 04-016-2015, blue vertical lines below the diffraction pattern). The Rietveld refinement operated in the hypothesis of a single phase evidenced a good agreement with the reference, however small but systematic shifts of the shape and position of the peaks were observed, and were attributed to the presence of a core-shell structure, synthesized in two steps.

EDX spectrum of CIS/ZnS-GSH QDs

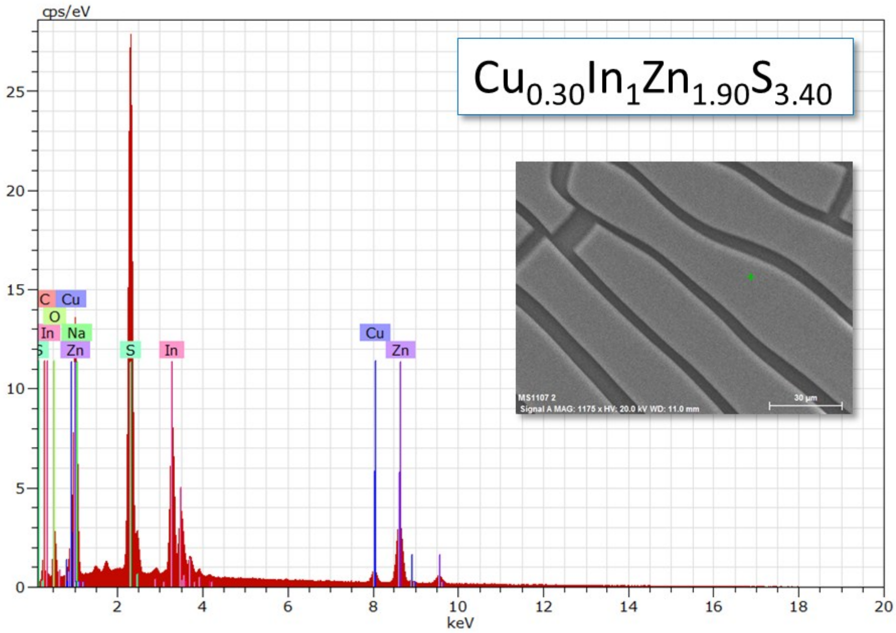

Figure S3. EDX spectrum of a CIS/ZnS-GSH nanocrystals sample dropcasted on a silicon substrate as a thick film. The composition was measured by EDX in five different points of the sample and the data were averaged to obtain the final values. The good thickness of the sample is proved by the fact that the Si signal is not observed in the spectra.

Thermogravimetric analysis of CIS/ZnS-GSH QDs

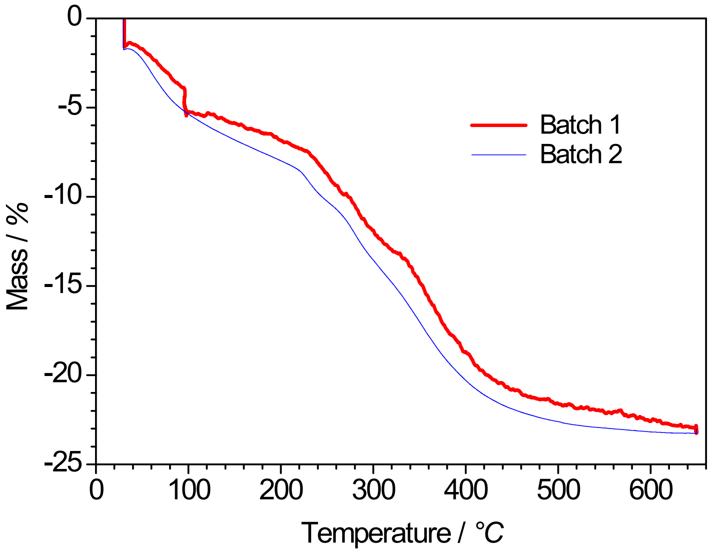

Figure S4. Thermogravimetric analysis of CIS/ZnS-GSH dry particles from two different batches, measured under argon atmosphere in a platinum crucible. The two batches gave similar results, confirming the good reproducibility of the synthetic procedure.

Emission lifetime of CIS/ZnS-GSH QDs in water

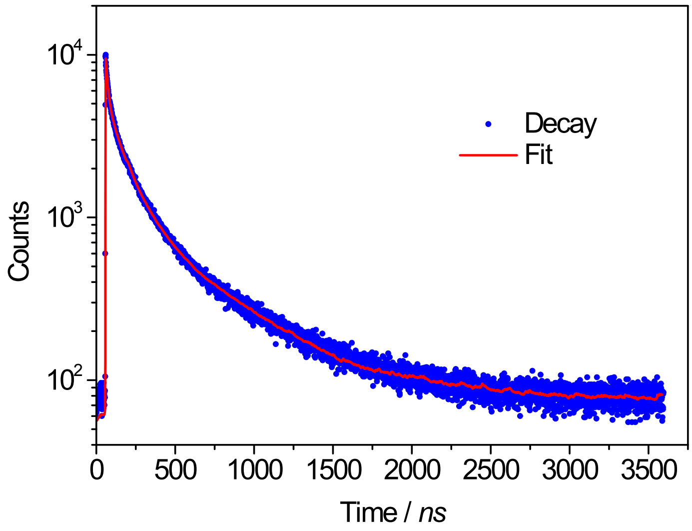

Figure S5. Emission decay for the CIS/ZnS-GSH QDs in aqueous solution, recorded at room temperature with a quartz cuvette of 1 cm. The solution was excited at 455 nm and the emission was recorded at 638 nm (integration time 0.1 s).

Table S1. Lifetime values obtained from a triexponential fit of the lifetime decay of CIS/ZnS-GSH QDIs in water as showed in Figure S5.

τ_1 / *ns*	A_1 / %	τ_2 / *ns*	A_1 / %	τ_3 / *ns*	A_1 / %	$\tau_{avg}{}^a$ / *ns*
13	6.36	100	37.61	371	56.02	328

[a] Average lifetime defined as $\tau_{avg} = (\tau_1^2A_1 + \tau_2^2A_2 + \tau_3^2A_3) / (\tau_1A_1 + \tau_2A_2 + \tau_3A_3)$

Estimation of the molar extinction coefficient of CIS/ZnS-GSH QDs

The mass concentration of the nanoparticles solution obtained after the synthesis (taking into account the residual water, removed at T < 100°C in thermogravimetric analysis, TGA) was:

$$C = 25 \text{ mg mL}^{-1}$$

The amount of ligands (mass %) was estimated from TGA to be around 15% (percentage of weight loss between 200 and 600 °C, see Figure S4). As a consequence, the mass concentration of the inorganic particles was:

$$c_{inorg} = 21 \text{ mg mL}^{-1}$$

The average nanoparticles size was obtained from TEM measurements: d = 2.2 nm. This corresponds to an average particle volume of 5.57×10^{-27} m^3 (inorganic part). Taking into account a density of 4.739 g mL^{-1} for bulk $CuInS_2$,[1] the average weight of a single inorganic particle (without considering the ligands) is

$$m_{inorg} = 2.64 \times 10^{-20} \text{ g}$$

which multiplied by the Avogadro number ($N_A = 6.022 \times 10^{23}$) can be considered as equivalent to the molar mass of $CuInS_2$ nanoparticles

$$MW_{inorg} = 15900 \text{ g mol}^{-1}$$

The molar concentration of the particles in the mother solution is thus obtained by the following equation:

$$C = c_{inorg} / MW_{inorg} = 1.32 \times 10^{-3} \text{ mol L}^{-1}$$

Knowing that the mother solution, diluted 1:61, has an absorbance $A_{400} = 0.4887$ at 400 nm (optical path b = 1 cm), the molar extinction coefficient at 400 nm (ε_{400}) can be estimated:

$$\varepsilon_{400} = \frac{A400}{b \times (Cinorg \div 61)} = 22600 \text{ cm}^{-1} \text{ M}^{-1}$$

This value is in the same range as those obtained for this size using two empirical formulae developed for stoichiometric $CuInS_2$ nanoparticles corroborating the validity of our estimation.[2,3]

Photocatalytic activities of the three-component systems SD-PS-Cat studied for H_2 evolution

Table S2. Photocatalytic activities of the three-component systems SD-PS-Cat studied for H_2 evolution, in terms of n_{H2}, TON_{Cat}, TON_{PS} and TOF_{PS}.[a] Experiments were carried out at 25 °C in water (5 mL) under visible-light (400–700 nm) with the NaHA/H_2A couple, as sacrificial electron donor (SD) and buffer, at different pH and with various relative concentrations of photosensitizer (PS) and catalyst (Cat).

Entry	pH	$[HA^-/H_2A]$ *(M)*	PS (*µM*)	Cat (*µM*)[b]	n_{H2}, *µmol*	TON_{Cat}	TON_{PS}	TOF_{QD}, *$mmol_{H2}$ g_{QD}^{-1} h^{-1}* (TOF_{PS}, *h*)	Irradiation time,[c] *h*
1	4.5	0.5	CIS/ZnS-GHS (102)	**Cat1** (10)	229	4580	900	1.80 (61)	69
2	5.0	0.5	CIS/ZnS-GHS (106)	**Cat1** (10)	295	5910	1110	1.59 (54)	97
3	5.5	0.5	CIS/ZnS-GHS (110)	**Cat1** (10)	244	4875	890	1.06 (36)	94
4	5.0	0.5	CIS/ZnS-GHS (117)	**Cat1** (5)	193	7720	660	1.02 (35)	98
5	5.0	0.5	CIS/ZnS-GHS (120)	**Cat1** (1)	47	9450	160	0.21 (7)	95
6	5.0	0.5	CIS/ZnS-GHS (114)		13		46		70
7	5.0	0.5	CIS/ZnS-GHS (117)	$Co(NO_3)_2$(10)	6.5	130	22		52
8	5.0	0.5	CIS/ZnS-GHS (116)	**Cat2** (10)	8.9	180	31		22
9	5.0	0.5	CIS/ZnS-GHS (68)	**Cat1** (10)	160	3200	940	1.33 (45)	71
10	5.0	0.5	$[Ru(bpy)_3]Cl_2$ (68)	**Cat1** (10)	32	640	190	(100)	30
11	4.5	0.5	$[Ru(bpy)_3]Cl_2$ (500)	**Cat1** (10)	80	1530	65	(35)	22
12	4.5	0.5	CdSe-GHS (68)	**Cat1** (10)	28	560	170	1.33 (45)	44
13	5.0	0.5	CdSe-GHS (5)	**Cat1** (10)	40	790	3155	25.53 (868)	93

[a] n_{H2}: total number of moles of H_2 produced; TON_{Cat}: maximum turnover number per catalyst (in mol_{H2} mol_{Cat}^{-1}); TON_{PS}: maximum turnover number per photosensitizer (calculated as $2 \times mol_{H2}$ mol_{PS}^{-1}); TOF_{PS}: initial turnover frequency per photosensitizer (expressed in mol_{H2} g_{QD}^{-1} h^{-1} or TON_{PS} h^{-1}) obtained by the system. [b] **Cat1** and **Cat2** correspond respectively to $[Co^{III}(CR14)Cl_2]Cl$ and $[Co^{II}(CR15)(H_2O)_2](Cl)_2$. [c] Time of irradiation after which H_2 production stopped or reached a pseudo plateau.

Table S3. Various concentrations of ascorbic acid (H_2A) and sodium ascorbate (NaHA) at different pH in aqueous solution.

pH	C */M*	$V_{solution}$ */mL*	$[H_2A]$/*M*	m_{H2A} */mg*	[NaHA]/*M*	m_{NaHA}/*mg*
4.5	0.5	5.0	0.142	125	0.358	354
5.0	0.5	5.0	0.056	49	0.444	440
5.5	0.5	5.0	0.019	17	0.481	476

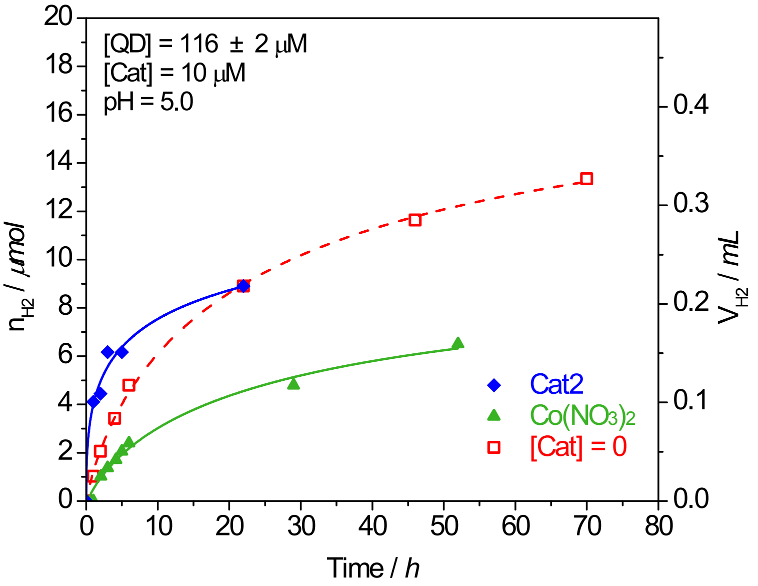

Figure S6. Photocatalytic hydrogen production (n_{H2}, V_{H2}) as a function of time from a deaerated aqueous solution (5 mL) of NaHA (0.36 M) and H_2A (0.14 M) at pH 5.0 under visible light irradiation (400-700 nm) in the presence of CIS/ZnS-GSH QDs (116 ± 2 µM) and in the absence (dashed line) or presence of catalyst (10 µM): **Cat2** ($[Co(CR15)(H_2O)_2](Cl)_2$, blue line) and $Co(NO_3)_2$ (green line).

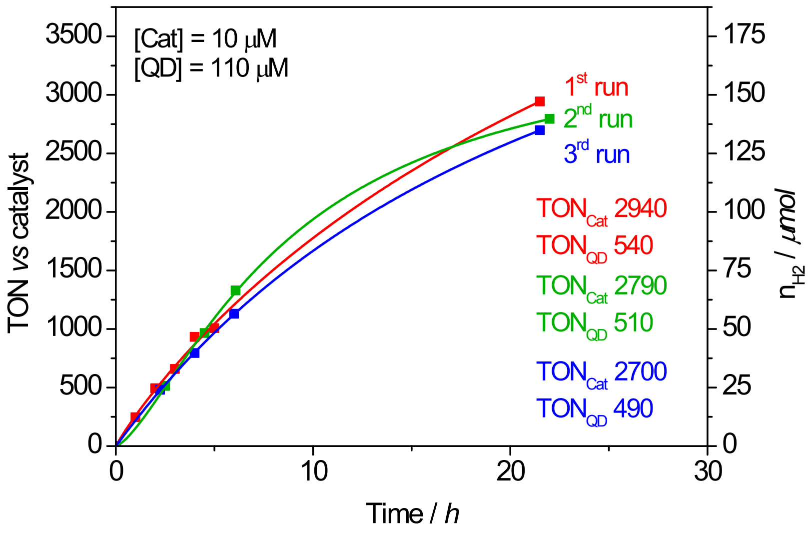

Figure S7. Photocatalytic hydrogen production (TON_{Cat}, n_{H2}) as a function of time from a deaerated aqueous solution (5 mL) of NaHA (0.36 M) and H_2A (0.14 M) at pH 5.0 under visible light irradiation (400-700 nm) in the presence of CIS/ZnS-GSH QDs (110 µM) and **Cat1** (10 µM) (1st run), after centrifugation and redispersion of CIS/ZnS-GSH QDs into a fresh solution of **Cat1** (10 µM) and NaHA (0.36 M)/H_2A (0.14 M) buffer (2nd and 3rd runs).

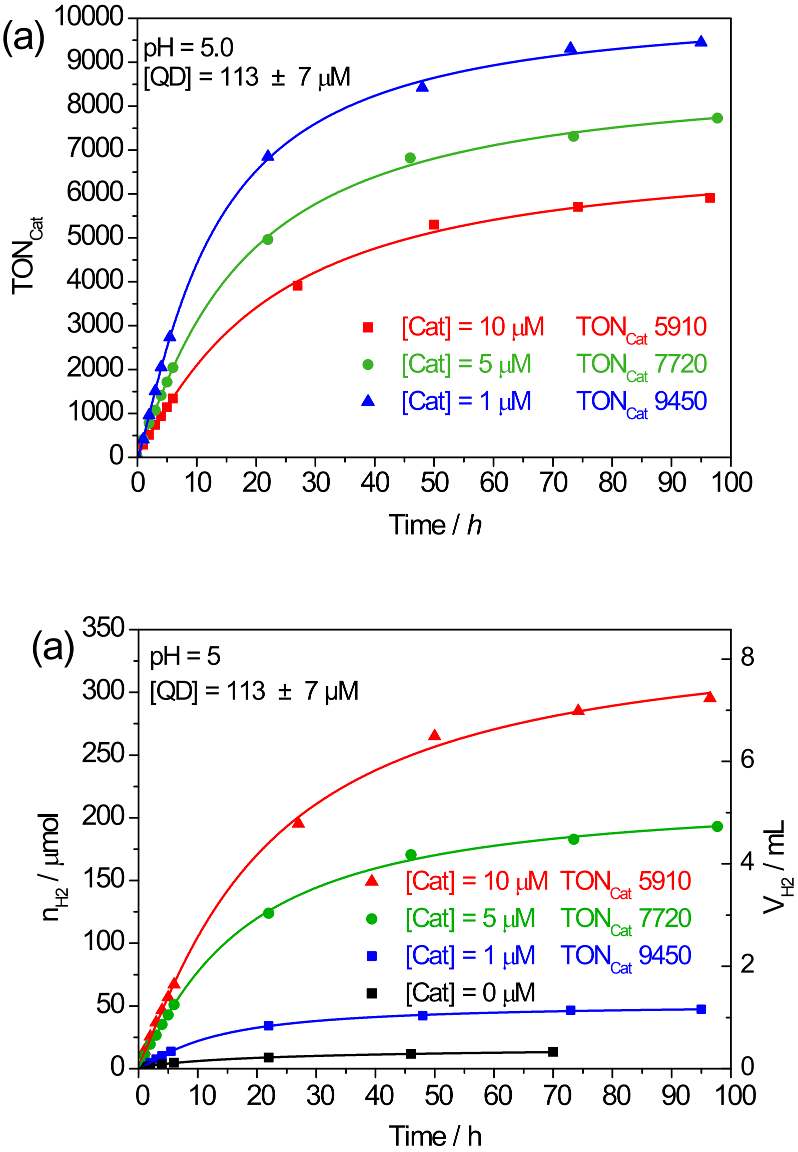

Figure S8. Photocatalytic hydrogen production as a function of time from a deaerated aqueous solution (5 mL) of NaHA (0.36 M) and H_2A (0.14 M) at pH 5.0 under visible light irradiation (400-700 nm) in the presence of CIS/ZnS-GSH QDs (113 ± 7 µM) and **Cat1** at different concentrations (1, 5, 10 µM) in terms of (a) TON_{Cat} and (b) n_{H2} and V_{H2}.

Spectral properties of CdSe QDs (synthesis and water transfer)

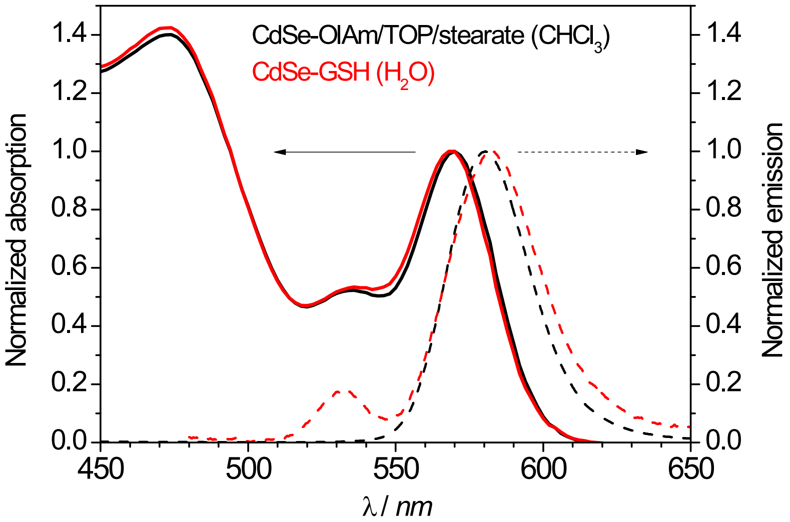

Figure S9. Normalized absorption (solid lines) and emission spectra (λ_{exc} = 400 nm) (dashed lines) of the CdSe QDs before (CdSe-OlAm-TOP-stearate, black line, recorded in chloroform) and after the water transfer (CdSe-GSH QDs, red line, recorded in water). The spectra do not exhibit significant shift after the water transfer, indicating that the properties of the nanocrystals were retained after the ligand exchange.

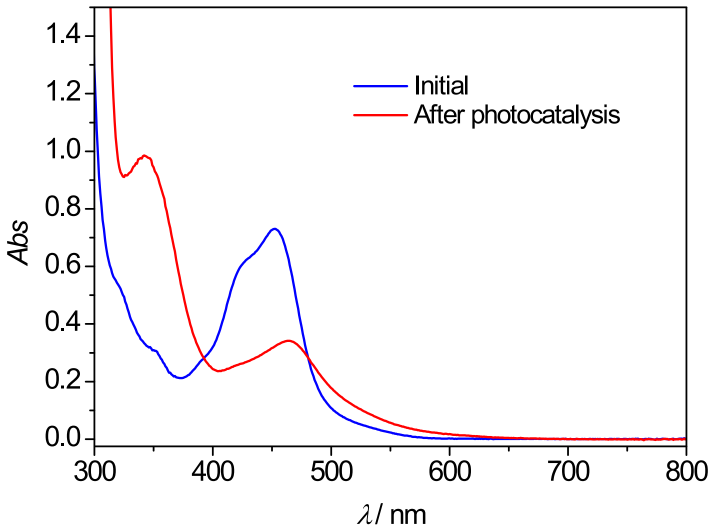

Figure S10. UV-Visible absorption spectra of an aqueous solution of $[Ru(bpy)_3]Cl_2$ (0.5 mM) and **Cat1** (5 µM) before adding ascorbic acid (▬), and of the mixture $[Ru(bpy)_3]Cl_2$ (0.5 mM), **Cat1** and $NaHA/H_2A$ (0.5 M) after photocatalysis (30 h of visible light irradiation) (▬). The spectra were recorded using a 1 mm path length quartz cell.

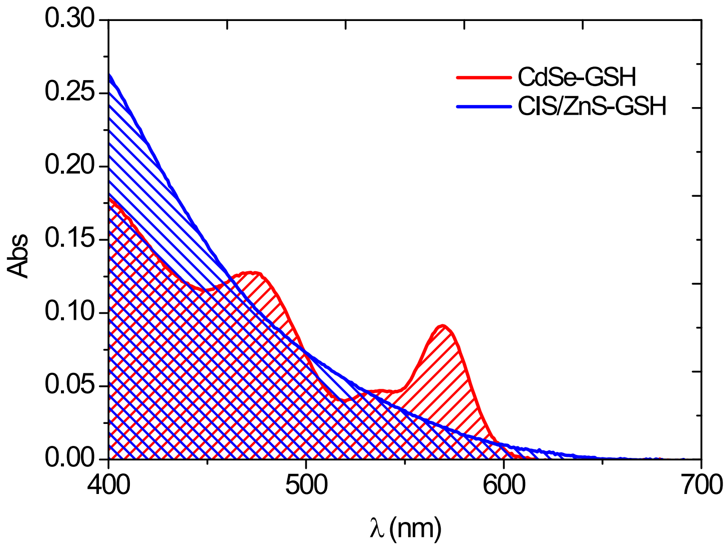

Figure S11. UV-Visible absorption spectra of (▬) the CIS/ZnS-GSH QDs (110 µM) and (▬) CdSe-GSH QDs (5 µM). The spectra were recorded in aerated water using a 1 mm path length quartz cell. The two spectra have the same area below the curve when integrated on the visible region of the spectrum (400-700 nm).

^{1}H NMR and mass spectra of [Co(CR14)Cl_2]Cl (Cat1) and [Co(CR15)(H_2O)$_2$]Cl_2 (Cat 2).

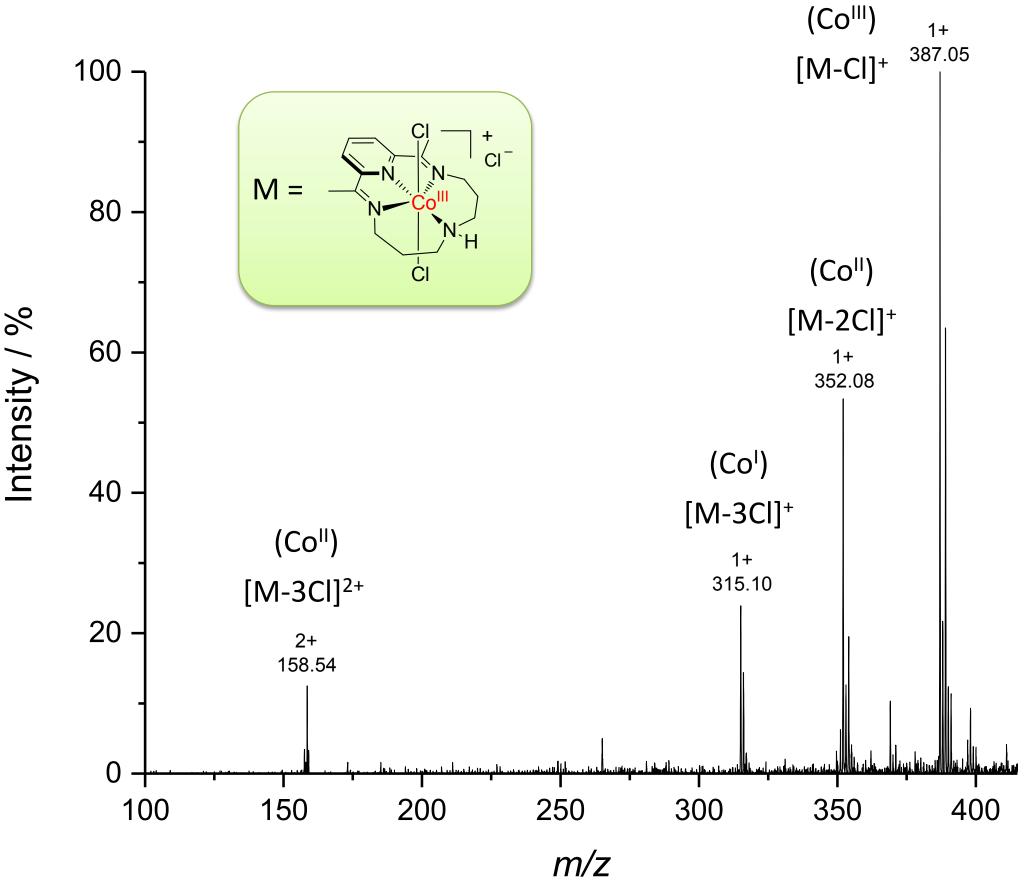

Figure S12. Positive ESI-MS spectrum of [Co(CR14)Cl_2]Cl (**Cat1**).

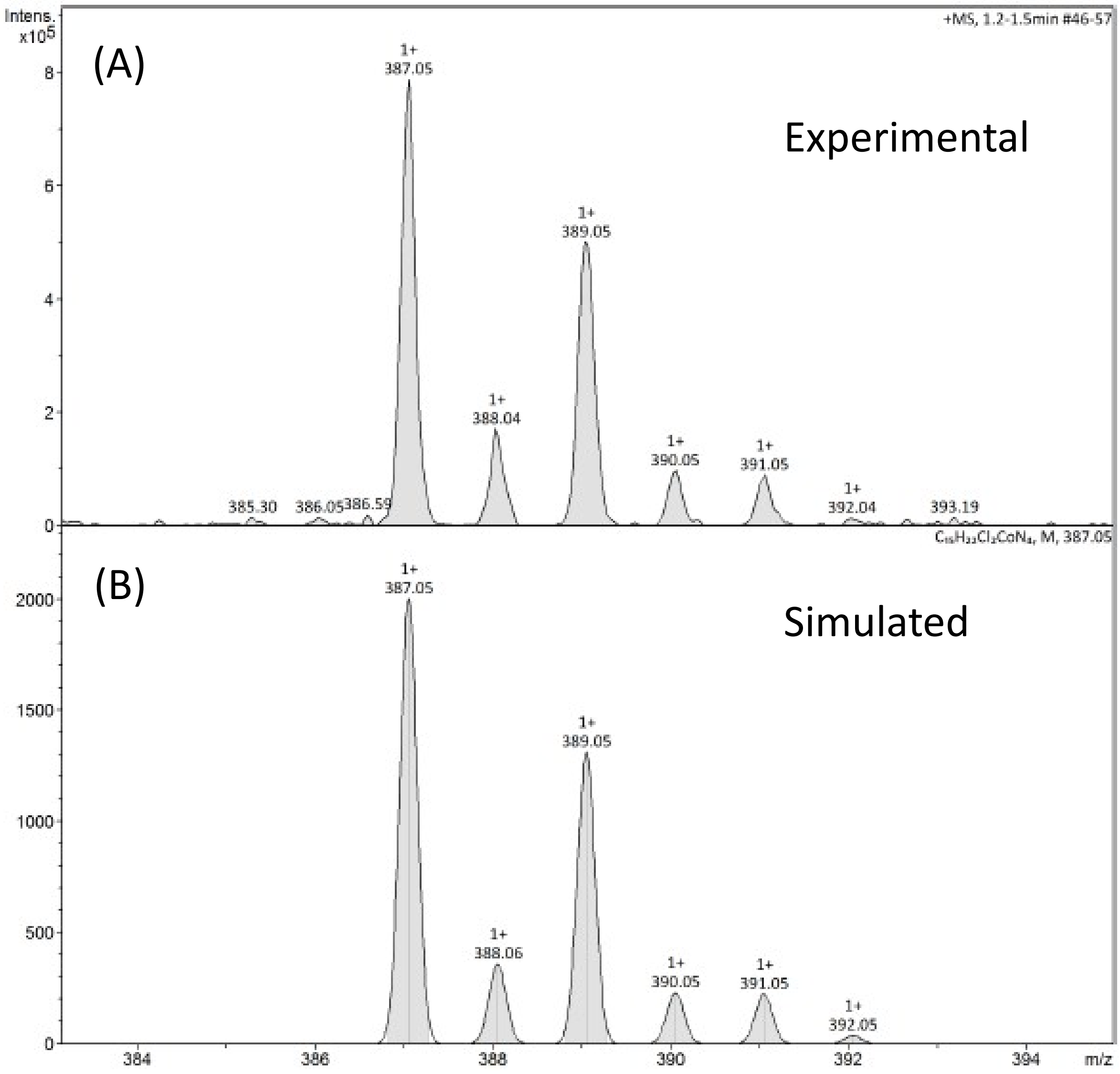

Figure S13. Peak expansion at *m/z* = 387.05 of the experimental ESI-SM spectrum of [Co(CR14)Cl_2]Cl (**Cat1**) (A) compared to the calculated isotopic profile for $[M-Cl]^+$ (387.05) (B).

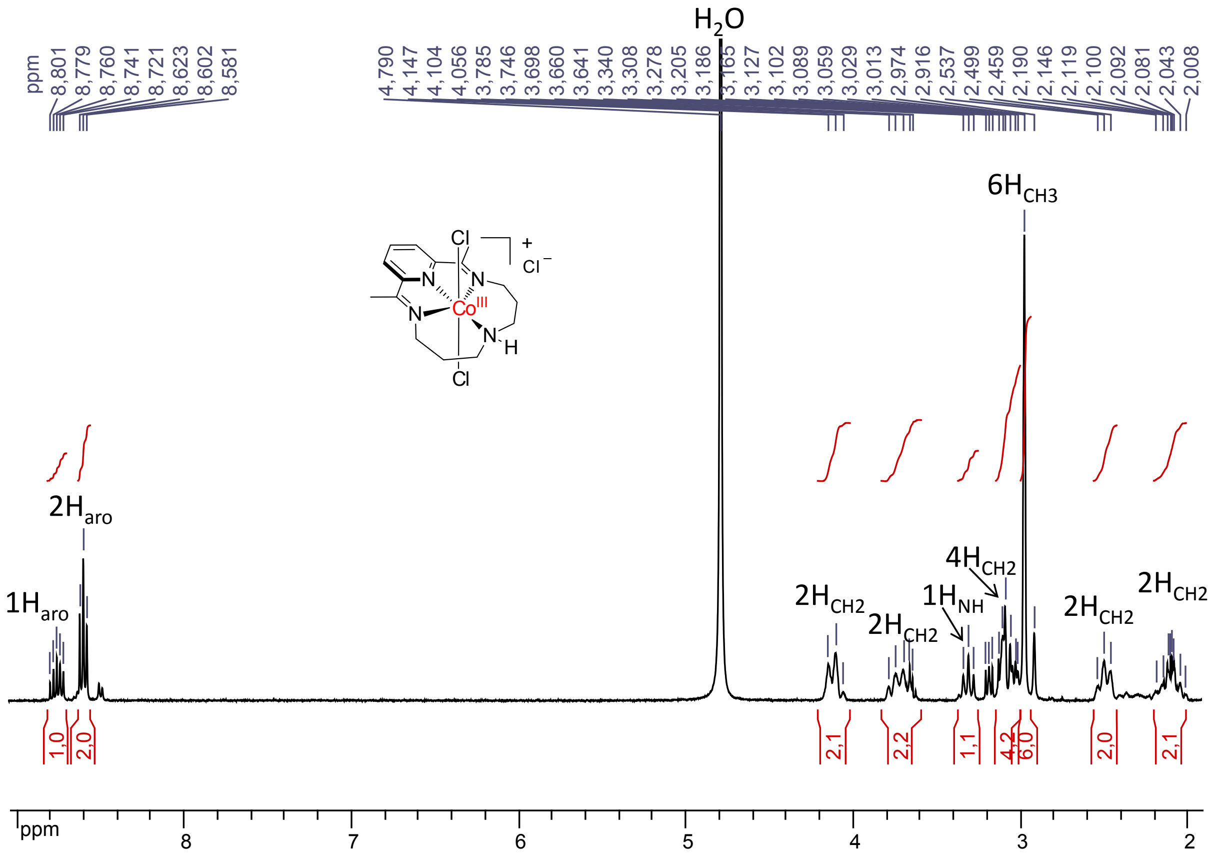

Figure S14. ^{1}H NMR spectrum (400 MHz) in D_2O of [Co(CR14)Cl$_2$]Cl (**Cat1**).

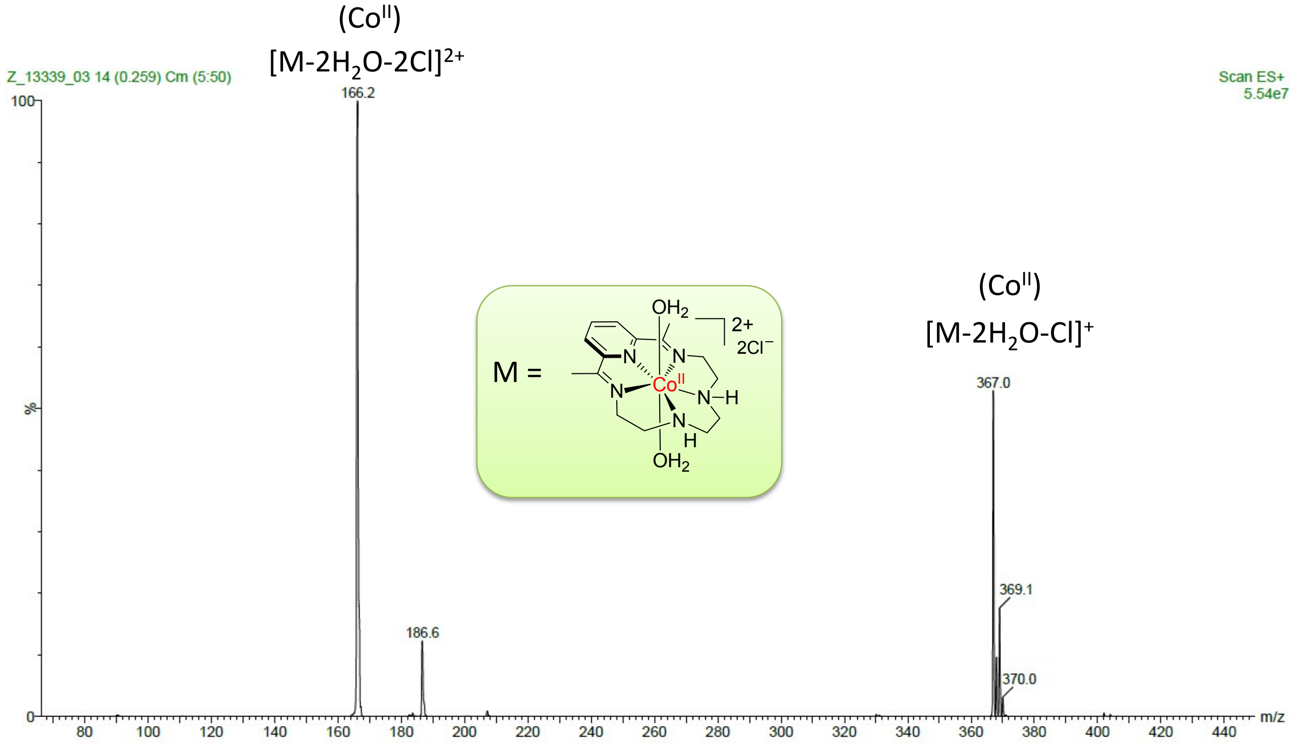

Figure S15. ESI mass spectrum of [Co(CR15)(H$_2$O)$_2$]Cl$_2$ (**Cat 2**).

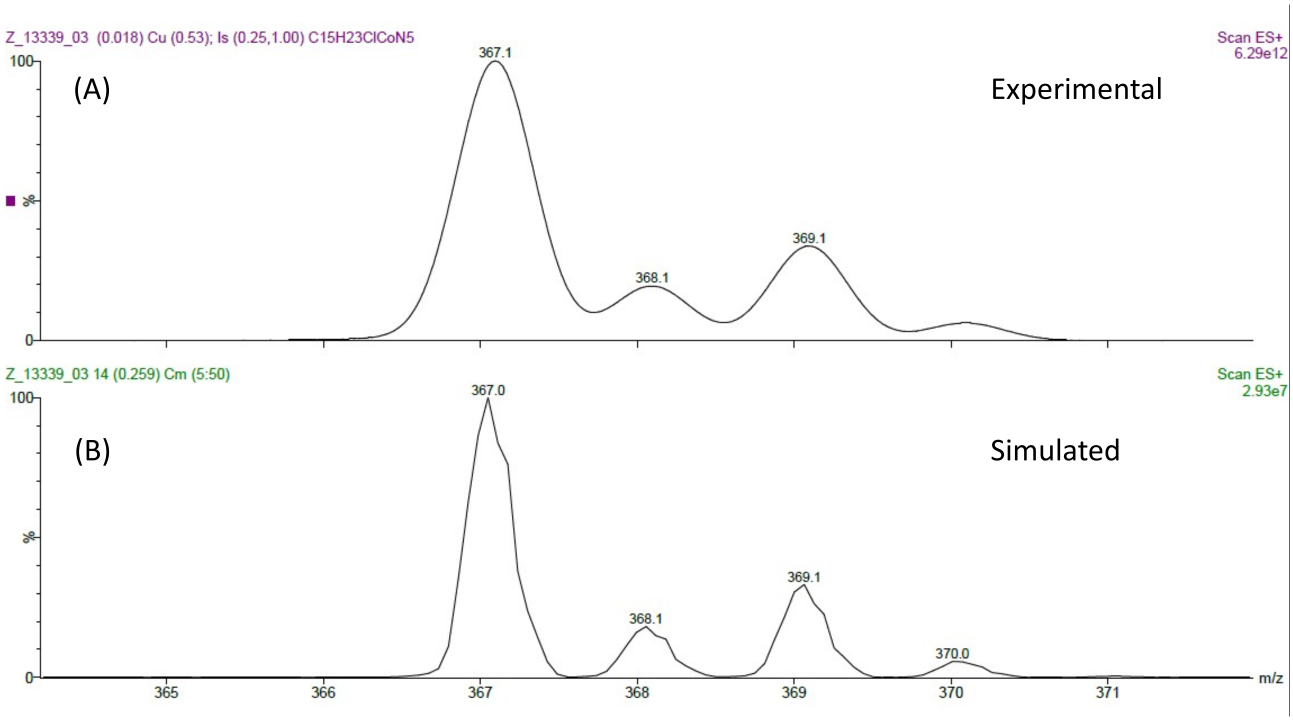

Figure S16. Peak expansion at *m/z* = 367.1 of the experimental ESI-MS spectrum of $[Co(CR15)(H_2O)_2]Cl_2$ (**Cat2**) (A) compared to the calculated isotopic profile for $[M\text{-}2H_2O\text{-}Cl]^+$ (367.097) (B).

References

(1) Akdas, T.; Walter, J.; Segets, D.; Distaso, M.; Winter, B.; Birajdar, B.; Spiecker, E.; Peukert, W. *Nanoscale* **2015**, *7*, 18105.

(2) Qin, L.; Li, D.; Zhang, Z.; Wang, K.; Ding, H.; Xie, R.; Yang, W. *Nanoscale* **2012**, *4*, 6360.

(3) Booth, M.; Brown, A. P.; Evans, S. D.; Critchley, K. *Chem. Mater.* **2012**, *24*, 2064.